Multiangle processing and multiscale characterization of walkaway VSP data

Jeroen Goudswaard, Menno Dillen and Kees Wapenaar, Centre for Technical Geoscience, Laboratory of Seismics and Acoustics, Delft University of Technology

Summary

In this paper a procedure is proposed for multi-angle imaging and elastic multiscale involved are: (1) a decomposition into up- and downgoing P- and S-waves; (2) compensation for the P- and S- downward propagation effects (inverse extrapolation); (3) imaging of the angle-dependent P-P and P-S reflectivity; (4) multiscale analysis of the imaged angle-dependent P-P and P-S data. It is shown that in the synthetic case, proper use of walkaway VSP data can improve the quality of the angle-dependent depth images, because internal multiples can be effectively suppressed when images of all receivers are combined. With real VSP data we will have an additional improvement, caused by the fact that the receivers are closer to the interfaces, which will decrease propagation related disturbances of the reflected wave-field.

Introduction of multiscale characterization

Multiangle, multiscale characterization on angle dependent seismic reflection responses was introduced by Goudswaard and Wapenaar (1997). For this characterization scheme an effective singular velocity profile was introduced that is consistent with multi-scale analyses of actual velocity well-logs, as analyzed by Herrmann (1997). This velocity profile, which is a generalization of step-function boundaries, consists of depth-shifted versions of

$$c(z) = \begin{cases} c_1|z|^{\alpha} & \text{for } z < 0 \\ c_2|z|^{\alpha} & \text{for } z > 0, \end{cases} \qquad (1)$$

in which α is the singularity parameter, and $c_{1,2}$ are factors that define the velocity contrast. It has been shown by Herrmann that estimates of α can be acquired by applying the Continuous Wavelet Transform (CWT) on a well-log, and by analyzing the amplitudes on so-called modulus-maxima lines in this wavelet-transformed data, closely following Mallat and Hwang (1992). Figure 1 shows an example of such an analysis on a synthetic velocity profile containing three distinct examples of a boundary described by eq. (1).

Furthermore, two distincts methods have been introduced to extract estimates of α from seismic reflection data migrated into rayparameter vs. depth ($p-z$)-gathers. The first method is discussed in Wapenaar et al. (1999); it is however only applicable to acoustic reflection responses.

The second method, including an analysis of the first method is described in Goudswaard (1999). In this method, first a linearized Zoeppritz inversion is performed (as developed by van Wijngaarden (1998)). The result of this inversion is a continuous estimate of the velocity contrast function $\Delta c(z)/\bar{c}(z)$, hereafter referred to as $D(z)$. From the self-similar relationship for velocity contrast functions the following relation for the amplitudes along modulus maxima lines was derived

$$\log(|\check{D}(\sigma, \sigma z)|) = (\alpha - 1)\log\sigma + \log(|\check{D}(1, z)|). \qquad (2)$$

Eq (2) implies that when a CWT is performed on this data, estimates of α can be acquired in the same way as they can be acquired from the well-log.

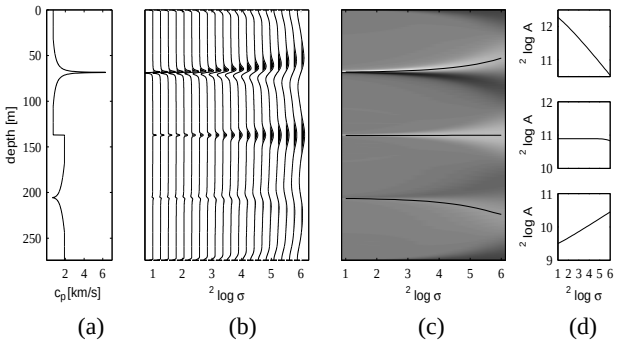

Fig. 1: *(a) Synthetic velocity profile with boundaries described by eq. (1)*
(b) Continuous Wavelet Transform of (a)
(c) position of modulus-maxima lines in wavelet transform
(d) log-log plot of amplitude along modulus-maxima lines vs. scale (top) $\alpha = -0.4$, (middle) $\alpha = 0$, (bottom) $\alpha = 0.2$

Multiangle processing of walkaway VSP data

In this paper we will apply these characterization methods on walkaway VSP data. be less than in surface data. Moreover, in the multi-scale analysis, the correlation of the results with well-logs will be much easier, since no time-depth conversion is required. The direct contribution in the downgoing P- and S-waves can be used to calibrate the generalized primary wave field extrapolation operators (that include dispersion related to the fine layering). These operators are used to acquire the multiangle imaging result. It is our intention to evaluate our elastic multiscale characterization method on a real walkaway VSP data set.

Since our characterization method has not been designed for walkaway VSP data, a number of adaptions is required, which we will briefly discusse here, at the hand of a numerical example. A typical multisource, multireceiver walkaway configuration is shown in Figure 2. Figure 3a shows a finely-layered target; Figures 3b and 3c show the v_x and v_z components of a walkaway VSP-experiment with the source at the surface, and receivers located at a depth of 391m.

First, a decomposition into up- and downgoing P- and S-waves

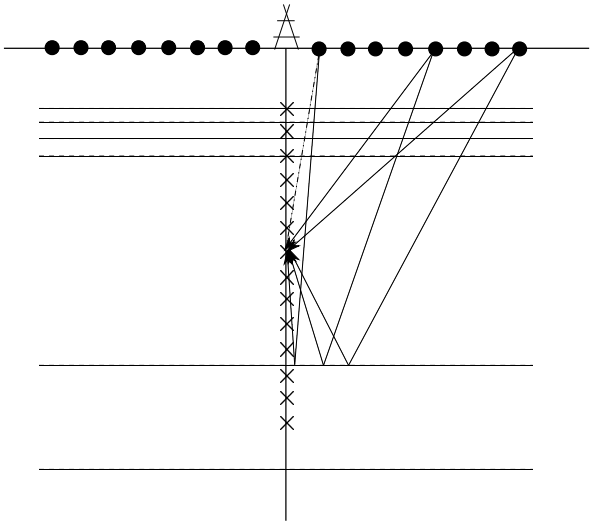

Fig. 2: *Multisource, multireceiver walkaway configuration.*

is required. To this end the walkaway VSP's (common receiver gathers) are reorganized into normal VSP's (common source gathers). In this domain the separation can take place by velocity filtering and polarization filters. A simulated decomposition result is shown in Figure 4a,b,c,d. Note that the direct contribution in the downgoing P- and S-waves (Figures 4a,b) can be used to calibrate the generalized primary wave field extrapolation operators (that include dispersion related to the fine layering). The decomposed data can be reorganized back into walkaway VSP's (common receiver gathers), see Figures 5a,b,c,d for a single receiver at z= 391 m and 16 sources at the surface. Note that the upgoing P- and S-components (Figures 5c,d) contain the angle-dependent response of the reflector package at the receiver depth.

After having performed this preprocessing, we have to image the angle-dependent P-P and P-S reflectivity, using the operators discussed above; in this example we will ignore the dispersion effects caused by the fine-layering. To this end, the data will be Radon-transformed into the rayparameter-intercept time $(\tau - p)$-domain. Note that analyzing data after a $(\tau - p)$-transform is only valid in the 1-D approximation. Because of the fact that in walkaway VSP data the receivers are very near to the interfaces, we can assume that this approximation is valid. Two imaging strategies are used to acquire the angle-dependent images R_{PP} and R_{PS}.

The first strategy is constructing a complete depth image $R(p, z)$ for a single receiver. Figures 6a,b show the result of this imaging strategy for the topmost receiver at 300m depth for the$P$-P and P-S data respectively. This imaging result clearly shows the main reflectors from the finely layered package, however it is blurred by many internal multiples.

The second strategy is constructing a complete depth image

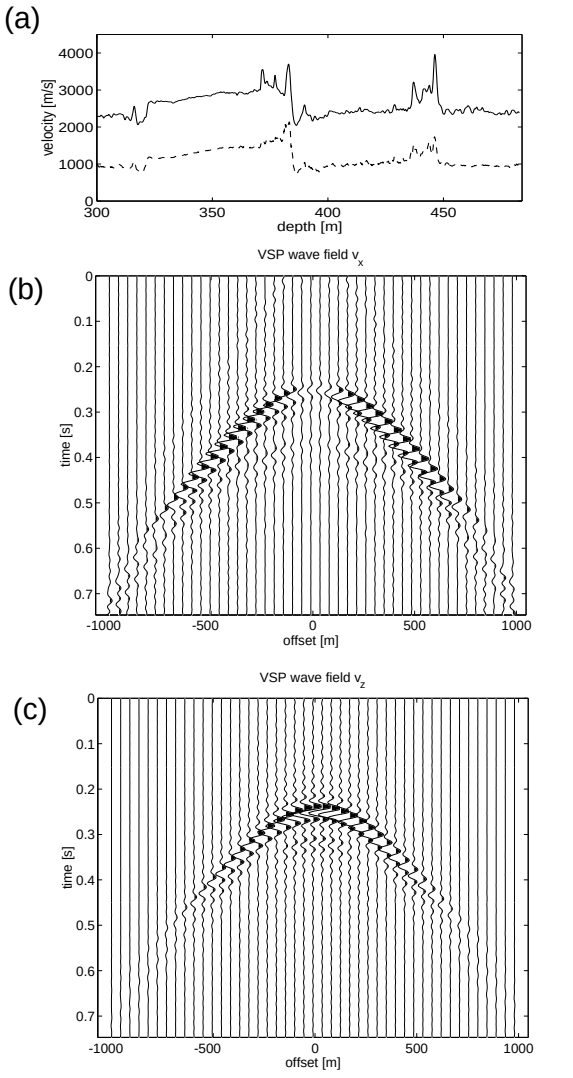

Fig. 3: *(a) Finely-layered target of the velocity profiles c_P (solid) and c_S (dashed) (b) v_x-component of the wave-field. (c)v_z-component of the wave-field.*

$R(p, z)$ by concatenating subimages from the receiver which is nearest to a specific depth in the image. By this technique we reduce the number of internal multiples in the image, because we will combine mainly the primary energy of all images. Figures 6c,d show the results of this technique. It shows that this imaging technique improves the resolution and decreases the amount of imaged internal multiples.

In the section on characterization we will analyze the images acquired by both imaging strategies.

Multiscale characterization of walkaway VSP data

The multiscale characterization on the imaged angle-dependent P-P and P-S in figure 6, will be performed according to the

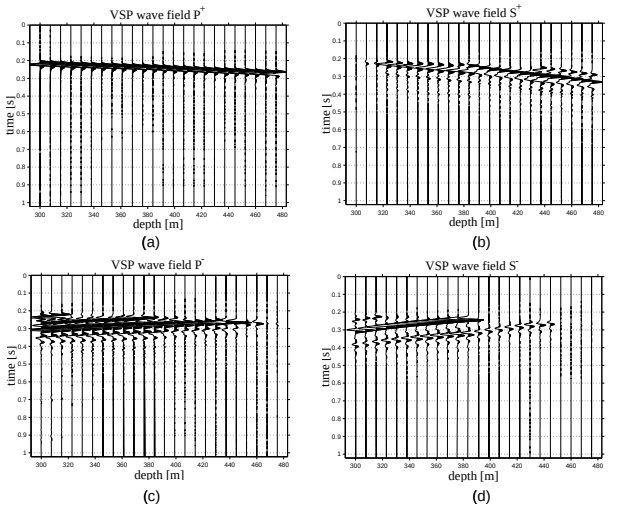

Fig. 4: *Common source VSP gathers. (a)P^+-component of the wave-field. (b)S^+-component the wave-field. (c)P^--component of the wave-field. (d)S^--component of the wave-field.*

approach discussed in the introduction. The goal is to show that estimates of semi-continuous α-profiles from well-log data are consistent with estimates from seismic reflection data.

First we have computed the α-profile of the P-wave velocity well-log of figure 3a. The result of this analysis is visible in figure 7a-d. The technique for this analysis was treated in the introduction to this paper. For the comparison between estimates of α from well-log and seismic data, we compute the profiles $D(z)$ from the data in figure 6, making use of the technique of Van Wijngaarden.

Figure 8a shows the estimate of $D(z)$ making use of the data

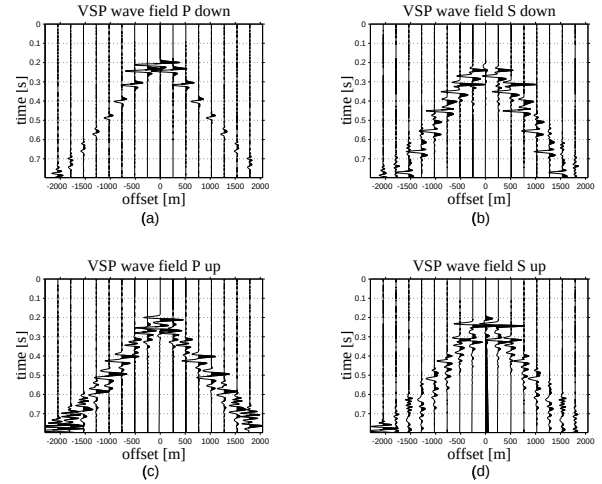

Fig. 5: *Common receiver VSP gathers with receiver at z= 391 m and 16 sources at the surface. (a)P^+-component of the wave-field. (b)S^+-component of the wave-field. (c)P^--component of the wave-field. (d)S^--component of the wave-field.*

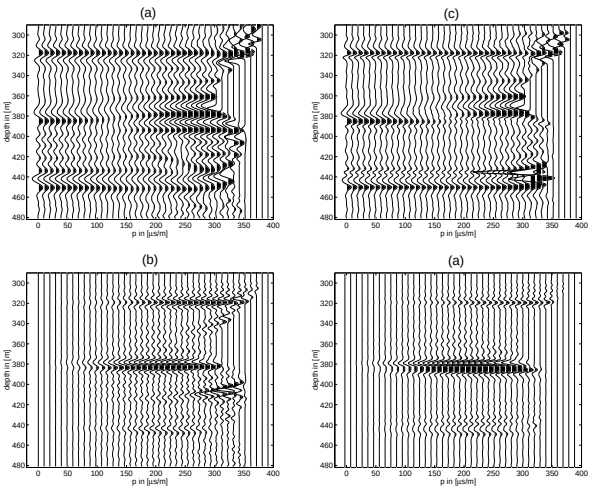

Fig. 6: *(a) Depth image $R_{PP}(p,z)$ for the receiver at 300m depth.*
(b) Depth image $R_{PS}(p,z)$ for the receiver at 300m depth.
(c) Depth image $R_{PP}(p,z)$ constructed by combining depth images of all receivers.
(d) Depth image $R_{PS}(p,z)$ constructed by combining depth images of all receivers.

sets in figure 6ab. Figure 9a shows the result acquired from the data sets in figure 6cd. Figures 8/9b,c,d show the results of performing the CWT on these data and extracting estimates of α from the depth image (the solid line in figures 8/9d.

It is clear from these pictures is that the $D(z)$-profile in figure 9a is much more pronounced than the one in figure 8a; it mainly shows the strong reflectors in the finely-layered package, whereas $D(z)$ in figure 8a seems to be affected by the multiple energy. The estimates of α from both data sets show that these estimates are less sensitive to this multiple energy, however the estimates from the data without multiple energy are more accurate than the results of the data constructed from the receiver at 300m depth.

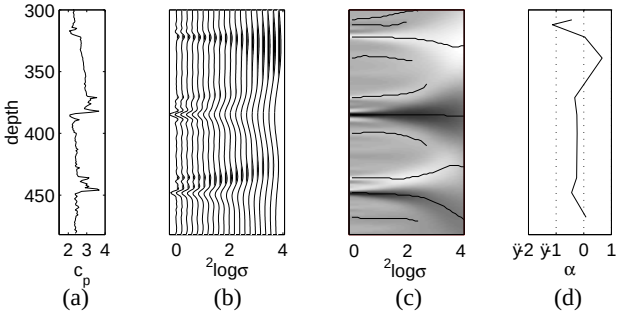

Fig. 7: *(a) P-wave velocity profile representing finely-layered target*
(b) Continuous Wavelet Transform of (a)
(c) position of modulus-maxima lines in wavelet transform
(d) estimates of α as a function of depth

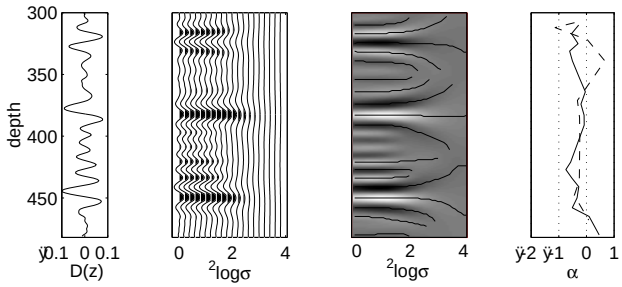

Fig. 8: *(a) Estimate of $D(z)$ from the seismic data in figure 6ab*
(b) Continuous Wavelet Transform of (a)
(c) position of modulus-maxima lines in wavelet transform
(d) estimates of α as a function of depth from $D(z)$ (solid) and from the P-wave velocity profile (dashed)

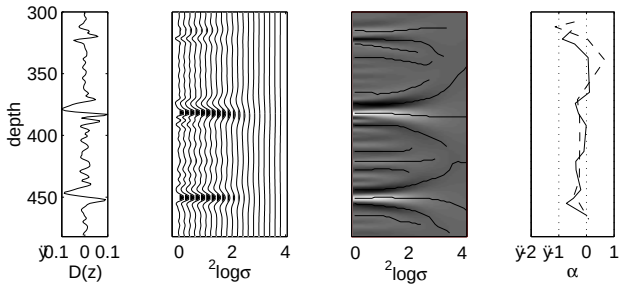

Fig. 9: *(a) Estimate of $D(z)$ from the seismic data in figure 6cd*
(b) Continuous Wavelet Transform of (a)
(c) position of modulus-maxima lines in wavelet transform
(d) estimates of α as a function of depth from $D(z)$ (solid) and from the P-wave velocity profile (dashed)

Conclusions

A multiangle, multiscale imaging and characterization method for walkaway VSP data has been proposed and analyzed on synthetic data. It was shown that from v_z and v_x measurements the data sets R^+_{PP}, R^+_{PS}, R^-_{PP} and R^-_{PS} can be constructed, which seem to contain no spurious events from other modes. These data sets have been the input of an imaging scheme in which VSP data from receivers at all depths were combined, to construct a depth image that has less internal multiples than the image from only one receiver. Both data sets have been analyzed by a multiangle, multiscale characterization method. A singularity parameter α-profile was extracted from a finely-layered package and from both these depth images. It was shown that the suppression of internal multiples in the imaging strategy enhances this inversion procedure. Current research involves the application of this method on real walkaway VSP data.

Acknowledgement The work reported here was supported under a grant from the Dutch Science Foundation STW (DTN 44.3547).

References

Goudswaard, J. C. M., and Wapenaar, C. P. A., 1997, Resolving well-log singularities from seismic data: 67th Annual Internat. Mtg., Soc. Expl. Geophys., Expanded Abstracts, 150–153.

Goudswaard, J., 1999, Multi-scale characterization of seismic reflection data: 61th Mtg., Eur. Assoc. Expl Geophys., Extended Abstracts, 4–56.

Herrmann, F. J., 1997, A scaling medium representation: Ph.D. thesis, Delft University of Technology.

Mallat, S. G., and Hwang, W. L., 1992, Singularity detection and processing with wavelets: IEEE Trans. Inform. Theory, **38**, no. 2, 617–643.

van Wijngaarden, A. J., 1998, Imaging and characterization of angle-dependent seismic reflection data: Ph.D. thesis, Delft University of Technology.

Wapenaar, C. P. A., Goudswaard, J., and van Wijngaarden, A. J., 1999, Multiangle, multiscale inversion of migrated seismic data: The Leading Edge, **18**, no. 8, 928–945.